Frequency- and time-resolved study of the dynamics of rubidium Rydberg wave packets in an electric field

G. M. Lankhuijzen and L. D. Noordam
FOM Institute for Atomic and Molecular Physics, Kruislaan 407, 1098-SJ Amsterdam, the Netherlands
(Received 20 January 1995)

The dynamics of an atomic wave packet in an electric field above the classical field ionization limit is studied in both the frequency and the time domain. We measure the photoionization yield of rubidium atoms in an electric field in the range 0.2–5 kV/cm as a function of the wavelength of the exciting laser. Fourier transforms of these spectra after multiplication with the spectrum of a short optical pulse allow us to make a direct comparison with time-resolved measurements performed by Broers *et al.* [Phys. Rev. A **49**, 2498 (1994)]. The dynamics of electronic wave packets above the classical field ionization limit as a function of the excitation energy is studied in detail, showing angular-momentum recurrences of the wave packet to the core on a picosecond time scale. The observed lifetimes up to 50 ps depend on excitation energy and polarization of the laser light. We also transform the frequency spectra to scaled-energy spectra, i.e., an alternative way of representing the dynamics of Rydberg wave packets. The frequency spectra allow us to compare the time-resolved spectra and the scaled-energy spectra directly. We find that near the saddle point ($\epsilon = -1.9$) radial and angular recurrences correspond to actions of $S = 0.77$ and $S = 2.4$, respectively. Just above the classical field ionization limit long-lived states are observed with lifetimes up to microseconds. These long decay times are measured in an alternative way: detection of the ionization yield as a function of time after the laser excitation.

PACS number(s): 32.60.+i, 32.80.Rm, 32.70.Fw

I. INTRODUCTION

Rydberg atoms are very well suited to study the dynamical behavior of electronic wave packets in electric fields. For these highly excited states the externally applied electric field can become comparable to the Coulomb field of the ionic core, allowing one to make a significant modification of the atomic potential. The modification of the atomic potential by an electric field is depicted in Fig. 1. The classical threshold energy above which the electron can classically escape over the saddle point of the potential is given by $E_c = -2\sqrt{F}$ (atomic units are used unless stated otherwise), where F is the electric field strength. In experiments in which states were excited around this classical field ionization limit, a detailed structure was observed in the ionization yield above E_c [1] indicating nonzero lifetimes of the excited states, which all have sufficient energy to escape from the Coulomb potential via the saddle point. Even above the zero-field ionization limit E_0 a modulation in the ionization yield has been observed for rubidium [2] and hydrogen atoms [3–5].

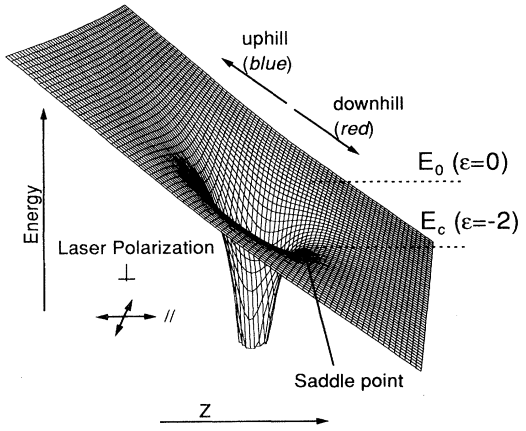

FIG. 1. Potential-energy surface of an electron in a combined Coulomb and electric field ($V = -1/r - Fz$). The classical ionization energy is lowered by the external electric field to $E_c = -2\sqrt{F}$. An electron with energy larger than E_c can escape over the saddle point.

In Fig. 2 the electronic energy levels of hydrogen in an electric field are plotted as a function of the electric field. The energy degeneracy of the l states is lifted when the atom is placed in an electric field. Angular momentum is no longer a conserved quantity. A projection onto a basis set consisting of parabolic k states, with fixed dipole moment, is made [6]. The energy of these so-called Stark states in first-order perturbation is given by

$$E = -\frac{1}{2n^2} + \frac{3}{2}nFk \ , \qquad (1)$$

where n is the principal quantum number, F is the electric field strength, and k is the parabolic quantum number with values $n-1, n-3, ..., -n+1$ for $m = 0$. The states increasing in energy as a function of the electric field are called "blue" states and correspond to states located "uphill" in potential (see Fig. 1). The states decreasing in energy, "red" states, correspond to states on the "downhill" side of the potential near the saddle point. In the hydrogen atom there is no coupling be-

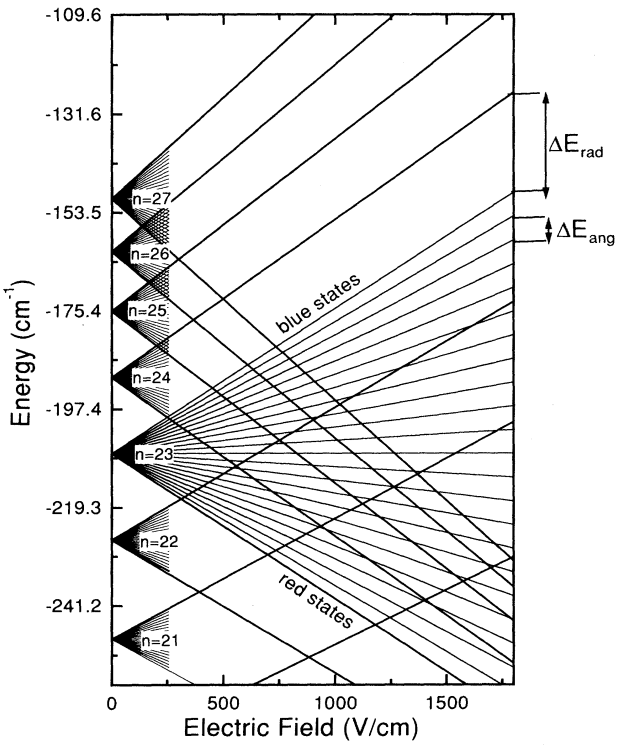

FIG. 2. Energy levels of electronic states of hydrogen as a function of the electric field. The l degeneracy is lifted by the electric field, giving rise to Stark manifolds for each principal quantum number n. The states with increasing energy are called "blue" states whereas the states that decrease in energy are called the "red" states.

tween the blue and red states. The extreme blue states are located far away from the saddle point and are therefore stable states even above the saddle-point energy. In alkali-metal atoms the blue and red states are coupled due to the core electrons [6]. Due to this coupling the blue states will also ionize, giving them a finite lifetime. Starting from the atomic ground state, Rydberg states can be excited by tunable lasers. The wave function that is excited by the laser will be dominantly located in the direction of the laser polarization. For a laser polarization parallel to the electric field the wavefunction will therefore be dominantly located in the z direction (see Fig. 1). In this case the extreme blue and red states, i.e., states with large $|k|$, are excited. For a laser polarization perpendicular to the electric field the wave function will be dominantly located perpendicular to the z axis corresponding to the middle Stark states in Fig. 2.

The dynamics of these short-lived states can be studied in the time domain. Short laser pulses with a bandwidth large enough to excite several eigenstates create an electronic wave packet. At energies above the classical field ionization limit the electronic wave packet can escape from the core over the saddle point (see Fig. 1), leading to ionization. Two types of wave packets can be distinguished. An angular wave packet is created when several Stark states belonging to one manifold are excited. The spacing between these states is given by $\Delta E = 3Fn$, corresponding to a beating time of $\tau_k = 2\pi/3Fn$. A radial wave packet is created when several states belonging to different n manifolds are excited with a beating time given by $\tau_n = 2\pi n^3$. The energy spacings of the states necessary to create radial ($\Delta E_{\rm rad}$) and angular ($\Delta E_{\rm ang}$) wave packets are depicted in Fig. 2.

Using a pump-probe technique bound wave packets have been studied extensively in the time domain [7,8]. Above the classical field ionization limit a pump-probe technique [9] has been applied for neutral atoms [10–12]. In these experiments a short laser pulse is used to excite a wave packet. After a delay τ_d a second identical pulse is applied to the atoms. By varying the phase between the two pulses, interference effects, giving rise to an enhancement or reduction of the Rydberg population, can occur only if the original wave packet has an overlap with the wave packet created by the second pulse. By measuring the amplitude of the interference as a function of the delay between the two pulses the recurrences of the wave packet to its original position and angular momentum can be measured directly. Starting from the $5s$ ground state of rubidium states are excited with p character ($l = 1$) using one-photon excitation. Since the excitation is above E_c the atom will ionize after some time. The ionization yield, which is equal to the final Rydberg population, is measured. The observable is given by $|\langle\Psi(0)|\Psi(\tau)\rangle|$, which is the overlap between the initial wave packet and the second wave packet that has been created after a delay τ_d. In this way the time evolution of the wave packet, appearing in the lifetime and the angular and radial recurrences of the wave packet, are measured [13,14]. For negative ions a similar detection technique is considered [15,16].

Scaled-energy spectroscopy provides a powerful tool for studying the dynamics of highly excited states in external fields. In these experiments the laser frequency, as well as the field strength, e.g., electric or magnetic, is scanned simultaneously to match the scaling criteria for the Hamiltonian describing the atom in the field. By Fourier transforming the spectra, individual periodic orbits can be unraveled. This method has been applied to atoms in both an electric [17–20] and a magnetic field [21,22]. The observed orbits were confirmed by classical periodic orbits calculations.

In this paper a third approach to study the atomic electron dynamics in an electric field is added to the two approaches discussed above. We present results from frequency-resolved spectra of rubidium in an electric field. Fourier transforms of these spectra after multiplication with the spectrum of a short optical pulse show the electron dynamics in the time domain as measured by the pump-probe experiment. The dynamics in an electric field above the classical field ionization limit is studied in detail and compared to scaling rules derived from the Stark splitting of the energy levels in an electric field. The energy spacing between levels in the frequency domain corresponds to "orbit" times of the electrons in the time domain. We observe features in the recurrence spectra that could not be unraveled using the pump-probe technique, showing that the frequency-resolved technique

is to be preferred in this case. The recurrence spectra are compared to time-resolved measurements performed by Broers *et al.* [14]. In the Appendix the analogy between the frequency, i.e., energy-resolved domain, and the time domain, is presented for the case of excitation of Rydberg states with a finite lifetime.

The link between radial and angular recurrences of the atomic electron wave packet in an electric field and the action spectra has not been discussed in detail up to now. Starting from the frequency spectra, we can generate both scaled-energy spectra and the time-domain evolution of the wave packet. This allows us to compare these two approaches directly and assign the action of classical orbits to radial and angular wave packets.

The outline of this paper is as follows. The experimental setup to measure the photoionization yield of rubidium in an electric field and the Fourier transform procedure is presented in Sec. II. In Sec. III a detailed study of the wave-packet dynamics as a function of the excitation energy between E_c and E_0 and the polarization of the laser is presented. The same analysis is applied to electronic wave packets of rubidium in an electric field of 4.3 kV/cm [2]. The exponential decay of long-lived states just above the classical field ionization limit is presented. A comparison between frequency-resolved experiments and time-resolved experiments by Broers *et al.* [14] will be made in Sec. V. In Sec. VI the link between the recurrence spectra and the scaled-energy spectra is presented.

II. FREQUENCY-RESOLVED IONIZATION OF RUBIDIUM IN AN ELECTRIC FIELD

A. Experiment

To measure the ionization yield of rubidium atoms in an electric field the following setup is used. In a vacuum system (10^{-5} Pa) a thermal beam of rubidium atoms from an oven passes between two condenser plates separated by 5.0 mm. The laser used for the excitation to the Rydberg states is a tunable nanosecond dye laser (bandwidth 0.1 cm^{-1}) that is pumped by the second harmonic of a Nd:YAG (where YAG denotes yttrium aluminium garnet) laser operating at 10 Hz. The output of the dye laser is frequency doubled in a potassium dihydrogen phosphate crystal and weakly focused in the interaction region, giving a maximum intensity of less than 10^6 W/cm^2. Starting from the $5s$ ground state of rubidium, the frequency-doubled output of the laser (ranging from 290 to 301 nm) is used to excite the Stark states by means of one-photon excitation. A positive voltage is applied to one of the condenser plates in order to obtain the electric field and to push the ions that are formed through a small hole (1 mm) in the other condenser plate towards a multichannel plate detector. The static field inhomogeneity in the laser focus is calculated to be less than 1%. The ion signal of the detector is monitored using a digital oscilloscope. A computer is used to read the oscilloscope and control the wavelength of the dye laser. The multichannel plate signal corresponding to the ionization yield and the laser intensity is monitored synchronously as a function of the laser wavelength. In this way variations of the laser intensity (less than 50%) caused by the doubling crystal and the gain curve of the dye laser are compensated. The linear response of the atomic excitation is checked by making scans at different intensities. No change in the spectra is observed for a laser intensity a factor 5 lower. The time window in the measurement of ionization is 200 ns, so only states with ionization rates faster than 200 ns are detected efficiently. The experimental resolution is determined by measuring the width of a long-lived Stark state just above the classical field ionization limit. The measured resolution is 0.6 cm^{-1}. Around the saddle-point energy, long-lived states are observed with lifetimes up to several microseconds. These lifetimes are measured by detecting the ionization yield as a function of time on an oscilloscope. The time resolution is 60 ns [full width at half maximum (FWHM)].

B. Fourier transform procedure

In Fig. 3(a) the measured ion yield as a function of the laser wavelength is plotted for rubidium in an electric field of 1.80 kV/cm. The laser polarization was chosen parallel to the electric field. We multiply this spec-

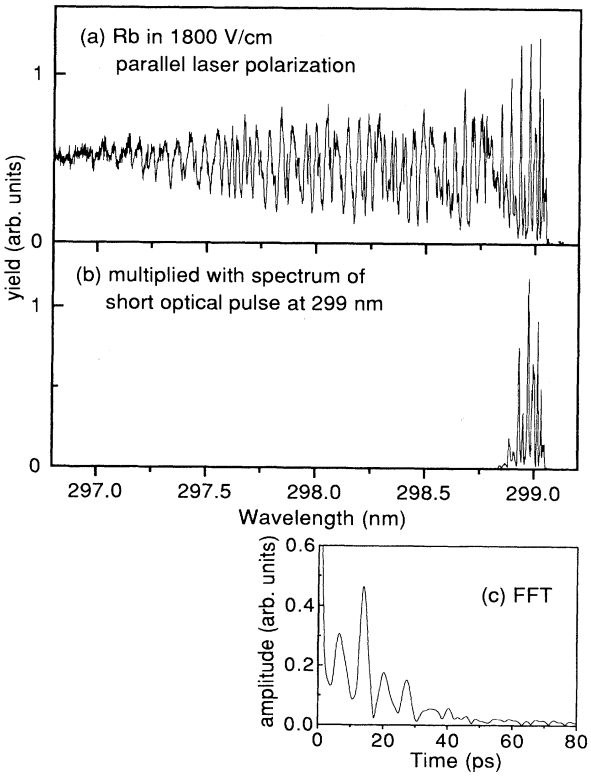

FIG. 3. (a) Ion yield as a function of the laser wavelength for rubidium in an electric field of 1.8 kV/cm. The laser polarization was chosen to be parallel to the electric field. (b) Same spectrum as in (a), multiplied with the spectrum of a 2.5-ps pulse that is used in a time-resolved measurement. (c) Fourier transform of spectrum (b).

trum with a Gaussian spectrum of a short optical pulse with a central wavelength of 299 nm [Fig. 3(b)]. This spectrum is Fourier transformed. In Fig. 3(c) the magnitude of this Fourier transform is shown. The pulse duration of the excitation pulse used in the experiments by Broers *et al.* [13,14] was found to be 2.5 ps (FWHM), giving a spectral width of 0.053 nm (FWHM) for a bandwidth limited pulse. We chose a slightly larger bandwidth 0.085 nm (FWHM) to match the actual bandwidth of the laser. The spacing between the dominant peaks observed in the Fig. 3(c) is proportional to the inverse of the Stark splitting of states belonging to one n manifold ($\Delta t = 2\pi/3Fn$). The bandwidth of the short laser pulse suffices to excite several levels within one n manifold. Therefore angular recurrences are observed. Each peak in Fig. 3(c) corresponds to a such a recurrence, so the vertical axis is given by the overlap between the two wave packets $|\langle\Psi(0)|\Psi(\tau)\rangle|$. In the left column of Fig. 4 the recurrence spectra that are obtained by Fourier transforming the frequency spectra are plotted next to the spectra that were obtained in a time-resolved wave-packet experiment by Broers *et al.* [14]. Various values of central wavelength of the pulses are chosen to excite wave packets between E_c and E_0. In Fig. 4 the laser polarization was chosen parallel to the electric field. Since the same experimental conditions are used, i.e., the electric field strength and the frequency of the laser, a direct comparison can be made between the time and frequency measurements (see the Appendix). In Fig. 5 the recurrence spectra are plotted for perpendicular polarization of the laser. The origin of the recurrences and the lifetimes of the wave packets will be discussed in Sec. III, while the comparison between the frequency and time-resolved method is postponed until Sec. V.

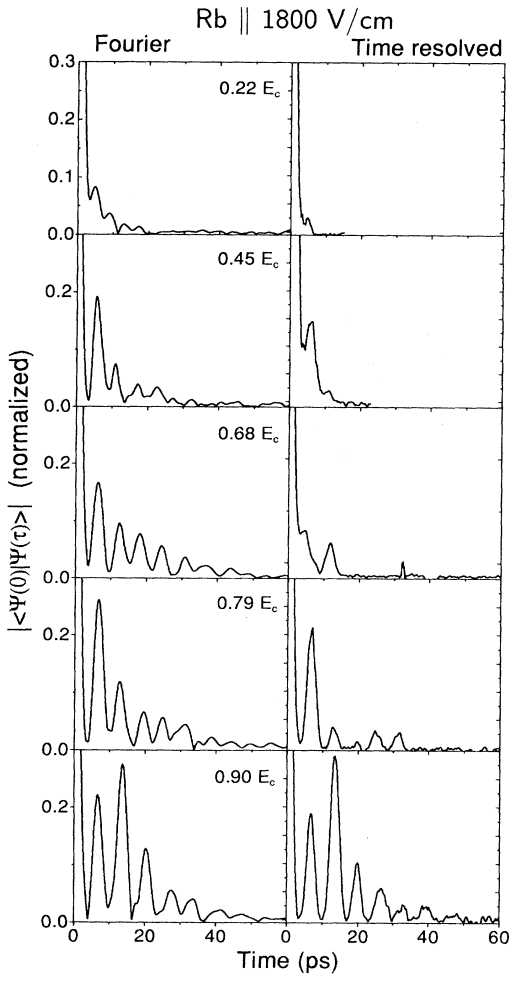

FIG. 4. The left column shows the recurrence spectra obtained by Fourier transforming a frequency-resolved spectrum of rubidium in 1.8 kV/cm for different values of the central frequency of the laser between E_c and E_0. The right column shows the same spectra obtained by a pump-probe wave-packet experiment by Broers *et al.* [14]. The laser polarization was chosen parallel to the static electric field. Vertical scale is normalized to the zero delay peak heights.

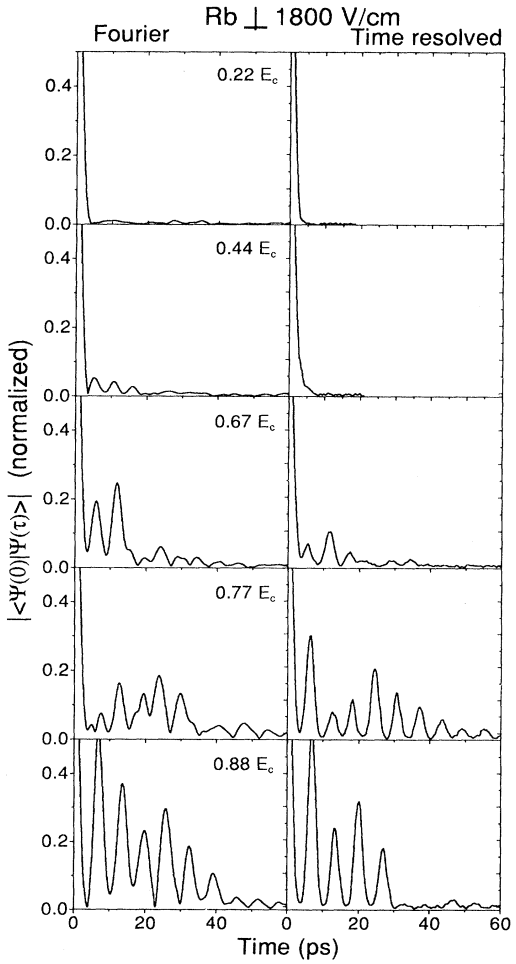

FIG. 5. Same as Fig. 4, but for laser polarization perpendicular to the static electric field.

III. DYNAMICS OF RYDBERG WAVE PACKETS ABOVE THE CLASSICAL FIELD IONIZATION LIMIT

A. Wave packets between E_c and E_0

The dynamics of the electronic wave packets that are created between the classical field ionization limit E_c and the zero-field ionization limit E_0 can be studied by analyzing the recurrence spectra. The observable in the recurrence spectra is the overlap between the initial wave packet and the wave packet that is created after a delay τ, i.e., $|\langle\Psi(0)|\Psi(\tau)\rangle|$. Since $\Psi(0)$ is excited from the rubidium $5s$ ground state by a short pulse, it will be located close to the core and have mainly p character. Therefore the part of the wave packet satisfying these two criteria after a delay τ will be measured. The lack of amplitude can be caused by one of the following reasons. Either the wave packet has escaped over the saddle point in the potential, i.e., field ionization has occurred, or the wave packet is still bound but has evolved to higher l states, which have no overlap with $\Psi(0)$. In the latter case the wave packet will return to its initial position and angular momentum after some time, giving an increase in the observed amplitude. This oscillatory behavior is called a recurrence of the wave packet. The overall lifetime of the wave packet can be seen from the decay of the peaks in the recurrence spectra. As the excitation energy exceeds E_c, the lifetime decreases for both polarizations (see Figs. 4 and 5). For the parallel polarization however, several recurrence peaks survive, even far above E_c. These recurrences are attributed to a wave packet that is "launched" uphill in the potential ($-z$ direction in Fig. 1) and returns to the core several times before the core has scattered the wave packet into the direction of the saddle point and field ionization occurs [23].

The bandwidth of the Gaussian pulse is large enough to excite several Stark states belonging to one n manifold. In this way an angular wave packet is created. The recurrence period is then given by the inverse of the energy spacing of the excited Stark states at this field strength. The spacing of the middle Stark states as a function of binding energy E and electric field strength F can easily be derived using the zero-field energy of $E = -1/2n^2$,

$$\Delta E_k(E,F) = 3nF = \frac{3F}{\sqrt{-2E}} , \tag{2}$$

and a corresponding recurrence time of

$$\tau_{\text{middle}}(E,F) = \frac{2\pi}{3}\frac{\sqrt{-2E}}{F} . \tag{3}$$

The Hamiltonian describing the atom in the electric field can be made independent of the electric field when scaled variables are introduced [20]. Using these scaled variables $\epsilon = E/\sqrt{F}$ can be derived, where ϵ denotes the scaled energy ranging from 0 at E_0 to -2 at E_c. The angular recurrence time for excitation of the middle Stark states is given by

$$\tau_{\text{middle}}(F) = \frac{2\pi\sqrt{-2\epsilon}}{3}F^{-3/4} . \tag{4}$$

For excitation of the bluest Stark states the expected recurrence time is given by

$$\tau_{\text{blue}}(F) = \frac{2\pi}{\sqrt{3\epsilon(1-\sqrt{1+3\epsilon^{-2}})}}F^{-3/4} , \tag{5}$$

giving a recurrence time of $\tau_{\text{blue}}(F) = 4.51F^{-3/4}$ at E_c and $\tau_{\text{blue}}(F) = 2.76F^{-3/4}$ at E_0. At E_c the recurrence time for the blue states is expected to be 8% longer than for the middle states. In Fig. 6 the experimentally obtained recurrence times at E_c ($\epsilon = -2$) as a function of the electric field are plotted for parallel (closed dots) and perpendicular (open dots) polarization. The dotted line is given by Eq. (4), which represents the expected recurrence time for excitation of the middle Stark states. The expected recurrence time for excitation of the bluest Stark states [Eq. (5)] is also plotted (full line). For hydrogen the excitation probability of the Stark components can be calculated [6]. For perpendicular polarization of the laser the middle Stark states (around $k = 0$) are dominantly excited. In the case of parallel polarization the reddest and bluest Stark states are dominantly excited. Since the red states are short lived, the recurrence time is mainly determined by the inverse energy spacing of the blue states. As predicted by Eqs. (4) and (5), the recurrence time for parallel polarization [blue states, Eq. (5)] is found to be somewhat longer.

In Fig. 7 the recurrence times are plotted as a function of the excitation energy, in units of E_c. The electric field is fixed at 4.3 kV/cm. Also shown in this plot is the expected recurrence time according to Eq. (4) (dashed line) and according to Eq. (5) (full line). The

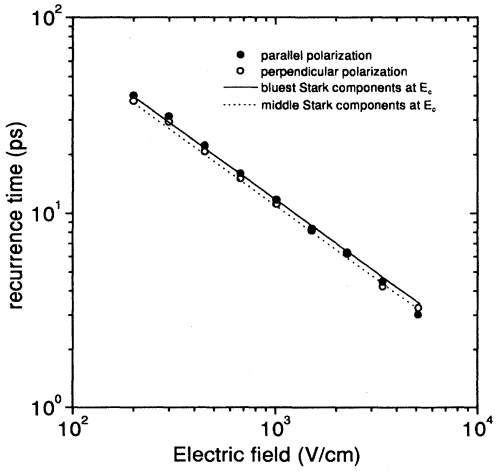

FIG. 6. Angular recurrence time as a function of the electric field at E_c. The closed dots are the experimentally observed recurrence times for laser polarization parallel to the electric field, and the open dots are for the perpendicular polarization. The full line gives the expected recurrence times for excitation of the bluest Stark states at 1.8 kV/cm at E_c [see Eq. (5)]. Also plotted are the expected recurrence times for the middle Stark states at 1.8 kV/cm at E_c [see Eq. (4)].

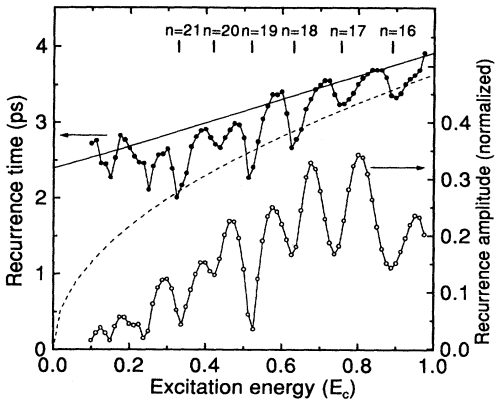

FIG. 7. Recurrence time (closed dots) and recurrence amplitude (open dots) of first recurrence as a function of excitation energy between E_0 and E_c in an electric field of 4.3 kV/cm. The laser polarization was chosen to be parallel to the electric field. The full line is the expected recurrence time for excitation of the bluest Stark components at this field strength. The dashed line is the expected recurrence time for the middle Stark components. Also plotted are the energy levels of the bluest Stark components at this field strength.

observed recurrences oscillate as a function of the excitation energy between the two lines. This indicates that the states that are excited vary from the blue to the middle Stark components. Also plotted are the positions of the bluest Stark components for hydrogen at this field strength. The period of the oscillation in the recurrence time coincides with the spacing between the bluest Stark components indicating that indeed the spacing between the Stark states that are excited is varying from the blue state spacing to the middle state spacing. Approaching E_0, the observed recurrence times tends more to the full line, i.e., the excited amplitude contributing to the first recurrence consists mainly of blue Stark states. The states that are excited oscillate from the middle Stark states to the blue Stark states as we go higher in excitation energy. Approaching E_0, only the blue states have a significant lifetime to give a structure in the frequency spectrum and hence contribute to the recurrences.

It is rather surprising that for an alkali-metal atom where all the states are strongly mixed in this regime the general trends in the dynamics of the wave packets can still be explained using the simple Stark formulas for hydrogen. The reason why this simple hydrogen model holds can be explained by the following argument. Due to the strong coupling the Stark states have avoided crossings. The energy of these states will therefore be different compared to the calculated hydrogen energies. However, the energy spacing between these states will be more or less unchanged. This energy spacing is determining the recurrence times of the wave packets. It appears that the strong coupling between these Stark states does not affect the character of the Stark state that much, i.e., the character of the blue states of hydrogen is still localized in a few Stark states in rubidium in this strong mixing regime.

In Fig. 8 the recurrence spectra between E_c and 0.5 E_0 are plotted for parallel and perpendicular polarization. A horizontal line gives the recurrence spectrum at a given energy E. The gray scale shows the amplitude of the recurrences $|\langle\Psi(0)|\Psi(\tau)\rangle|$. A number of interesting features appear in these spectra. As the energy increases the recurrences die out, indicating the decrease in lifetime of the wave packet. Furthermore, the amplitude of the first recurrence oscillates as a function of the excitation energy. For the parallel excitation the spacing between these oscillations is equal to the spacing between the bluest Stark components of the n= 20–22 Stark manifolds at a field strength of 1.8 kV/cm.

At $0.65E_c$ and $0.76E_c$ a local minimum is found in the first recurrence amplitude. The amplitude of the second

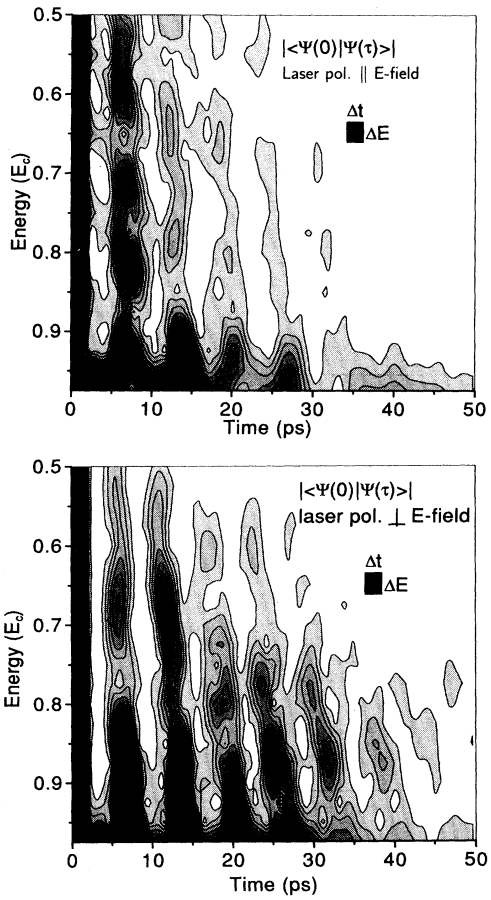

FIG. 8. Recurrence spectra for rubidium in an electric field of 1.8 kV/cm as a function of the excitation energy between E_c and E_0. The laser polarization was chosen to be parallel (upper graph) and perpendicular (lower graph) to the electric field. The gray scale is changing linearly from 0 to 0.355 (black above 0.355). The spectra are normalized to the amplitude of the zero delay peak. The first angular recurrence at about 7 ps shows an oscillatory behavior as a function of the excitation energy. The spacing between these peaks for parallel polarization corresponds to the spacing between the bluest Stark components of the n = 18, 19 Stark manifolds at a field of 1.8 kV/cm.

recurrence is higher in this region. In terms of closed orbits this can be explained as follows. The orbit of the electron is not completely closed after one round-trip, i.e., it narrowly misses the core, giving a small recurrence amplitude. After the second round-trip the orbit is closed, giving a higher recurrence amplitude.

The spectral width that is Fourier transformed is chosen in such a way that on both axes, i.e., energy and time, the same amount of structure can be observed. If the spectral width was chosen to be larger than 0.085 nm (FWHM), more structure will be observed in the time domain but less structure in the energy domain, satisfying the Heisenberg uncertainty principle $\Delta E \Delta t = 2\pi$. The black square in Fig. 8 shows this area (multiplied by 0.4 for the FWHM of a Gaussian pulse).

B. Rubidium in an electric field of 4.3 kV/cm

In this section the ionization yield of rubidium atoms in an electric field of 4.3 kV/cm will be discussed. In the pioneering experiments by Freeman *et al.* [2] a modulation in the ionization yield above the zero-field ionization limit was observed for rubidium at this field strength. The resolution of our spectrum (0.6 cm^{-1}) is comparable to that measured by Freeman *et al.* (0.5 cm^{-1}). Here we will Fourier transform this spectrum and focus on the dynamics rather than the spectral behavior.

In Fig. 9 the ionization yield of rubidium in an electric field of 4.3 kV/cm as a function of the wavelength is shown. Instead of trying to make a level by level analysis of this spectrum, the Fourier transforms of this spectrum multiplied by Gaussian pulses is taken at a number of wavelengths. In Fig. 10 a contour plot of the recurrence spectra as a function of the excitation energy between E_c and E_0 is plotted.

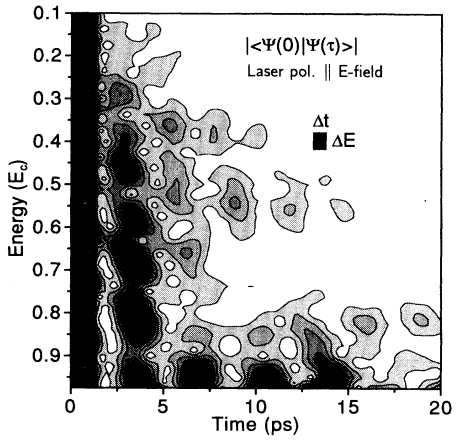

FIG. 10. Recurrence spectra as a function of excitation energy between E_0 and E_c at 4.3 kV/cm. The spectrum is normalized to the zero delay peak. The contour scale is varying linearly from 0 to 0.35.

Note the striking, but unexplained, lack of recurrences near $E = 0.7E_c$. In Fig. 11 the spectrum of Fig. 9 is convoluted with a Gaussian of 0.166 nm FWHM. In this figure we observe a modulation of the ionization yield as a function of the excitation energy. The modulation period corresponds to the spacing between the bluest Stark components of the n = 16–18 manifolds at 4.3 kV/cm (calculated up to second-order perturbation). For comparison, the field free Rydberg levels are plotted as well. The dotted line in Fig. 11 gives the recurrence amplitude of the Fourier transformed spectrum of the first recurrence at 3.5 ps.

We will now discuss the origin of the oscillations in Fig.

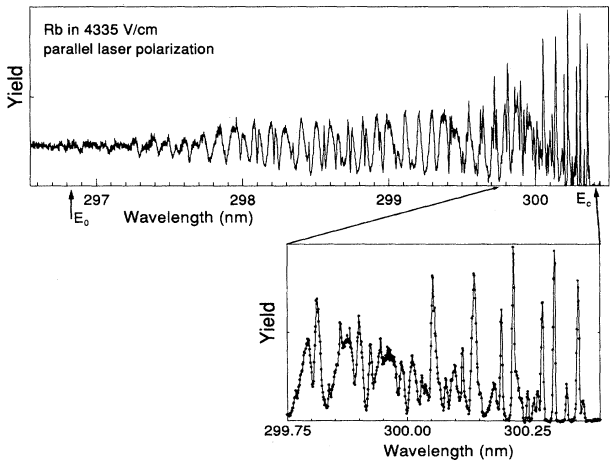

FIG. 9. Ionization yield of rubidium in an electric field of 4.3 kV/cm as a function of the wavelength. The laser polarization was chosen parallel to the electric field. The upper graph shows a blowup of the spectrum from 299.5–300.5 nm.

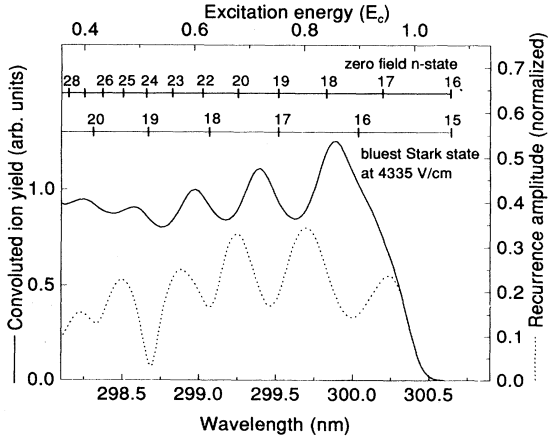

FIG. 11. Ionization yield of rubidium in an electric field of 4.3 kV/cm convoluted with a Gaussian of 0.166 nm FWHM. The laser polarization was chosen to be parallel to the electric field. The spacing between the energy levels of the bluest Stark components of n = 15–20 at 4.3 kV/cm corresponds to the spacing between the maxima in the convoluted spectrum. For comparison the zero-field n states are also plotted.

11 both in the convoluted spectrum and in the recurrence amplitude. Although a quantum analysis of rubidium in an electric field is required for a complete understanding, a qualitative description can be given by an inspection of the energy levels for hydrogen. For the analyses only the bluest Stark states are of interest since the other Stark states contribute to the continuous background because of their short lifetime corresponding to a large width of the resonances. The hydrogenic energy levels of these blue Stark states are calculated using the Stark effect up to second order. The Stark manifolds overlap at this field strength. For instance, only the three bluest members of the $n = 18$ manifold are at higher energies than the bluest member of the $n = 17$ manifold. Analyzing Fig. 11, we observe that the spacing between the bluest Stark components at this field strength is equal to the modulation period in both the convoluted spectrum and the recurrence amplitude. From the spacing between the oscillations in the convoluted spectrum we see that the blue character is still localized in a few eigenstates; otherwise a flat spectrum would be expected. An enhancement of the excitation probability is expected at the spectral location of the blue states. The exact position of the oscillations of the ionization cross section is not in agreement with the calculated levels. This is no surprise since the blue character of the rubidium Stark states in this strongly coupled regime is not located at the same spectral position as in the case of hydrogen. Intuitively one expects the highest recurrence amplitude at spectral positions where long-lived blue states are localized. However, a shift is observed in the oscillation of the recurrence amplitude. This shift is unexplained and urges a full quantum analysis. By Fourier transforming the spectra we have a tool to separate the contribution of short-lived red states, which appear only in the zero peak, from the surviving blue states, which appear in the recurrences.

C. Detection of long-lived Rydberg states at E_c

For laser excitation just above E_c long-lived states are observed with lifetimes up to microseconds. In the frequency domain, the bandwidth of the exciting laser needed to resolve a state with a lifetime of 1 μs has to be very small (less than 0.5 MHz). Using a continuous dye laser, a bandwidth of 1 MHz has been obtained [22]. In experiments where atoms were excited with this laser a residual Doppler width of 25 MHz was measured [22]. The experimental spectral resolution in our setup corresponds to a bandwidth of 18 GHz, making it impossible to resolve the linewidth of these long-lived states. However, the pulse duration is short (less than 10 ns) with respect to this lifetime, allowing us to study the dynamics of these states in the time domain.

In Fig. 12 such a direct lifetime measurement is plotted. The ionization yield was measured as a function of time with a channel plate detector and a fast oscilloscope. Two different resonances were excited just above the classical field ionization limit at $0.972E_c$ and $0.978E_c$. The laser polarization was parallel to the electric field of

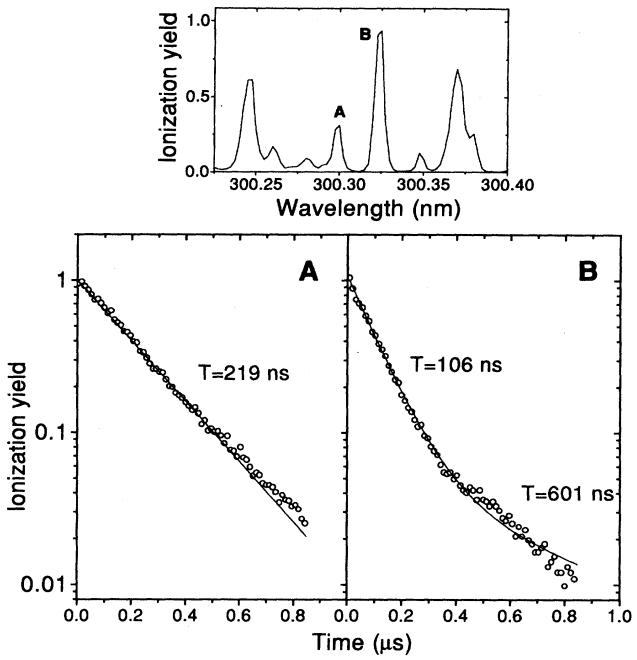

FIG. 12. Measured exponential decay (dots) after excitation of Rb in an electric field of 4.3 kV/cm just above the classical field ionization limit E_c. The laser polarization was chosen to be parallel to the electric field. In the left figure the excitation was at 300.300 nm. A single exponential decay is fitted to these points giving a decay time of 219 ns. In the right figure the excitation was at 300.325 nm. A double exponential decay is observed with lifetimes of 103 ns and 600 ns.

4.3 kV/cm. In the left figure an exponential decay with a lifetime of 219 ns is observed. In the right figure a double exponential decay with lifetimes of 106 ns and 601 ns are observed. This double exponential decay can be explained by the large bandwidth (3 GHz) of the nanosecond dye laser. Within the bandwidth of the laser more than one state is excited, giving rise to this double exponential decay. The nanosecond dye laser used here is not a single mode laser; otherwise the bandwidth would be less then 0.5 GHz, given by the inverse of the pulse duration. The output of the laser consists of many different longitudinal modes giving rise to this larger bandwidth. The two states that are excited are most likely excited by different modes within the laser pulse.

These data show that just above E_c some states are very long lived. To study these states in full detail, neither frequency- nor time-domain experiments are useful. The time-domain pump-probe experiments are impractical since 1 μs corresponds to an optical delay of 300 m. Frequency-domain measurements at a sub-megahertz level suffer from Doppler width. Most convenient seems a combined time- and frequency-domain effort: using a narrow band pulsed dye laser to ensure excitation of a single state and monitoring the atomic decay in the time domain.

IV. COMPARING FREQUENCY- AND TIME-RESOLVED MEASUREMENTS

In the frequency-resolved measurement the same experimental condition were chosen as the time-resolved measurements performed by Broers *et al.* [13,14] to allow for a direct comparison. In Figs. 4 and 5 the Fourier transformed frequency- and time-resolved measurements are plotted for parallel and perpendicular laser polarization, respectively. Comparing the two sets of data leads to the following conclusions. First, the positions of the recurrence peaks are in good agreement with each other for all excitation energies, as can be seen in Table I. Second, the general trend that farther above E_c the total number of recurrences decreases for both polarization is observed in both data sets. For the parallel polarization one recurrence survives even far above E_c, corresponding to a wave packet that moves uphill in the potential, as can be seen in Fig. 1, which is observed in both cases. Third, the relative peak heights show good agreement for the parallel polarization, but some discrepancies for the perpendicular polarization measurements are found.

We will now discuss the differences in the two types of experiment. In the frequency domain measurements, the frequency resolution of the laser determines the maximum time in which the structure can be observed. A spectral resolution of 0.6 cm^{-1} corresponds to a time of 55 ps. For the wave packets examined here the life time is less than 55 ps, so the spectral resolution is good enough to observe the evolution of the wave packet. Using a continuous wave dye laser, a much smaller bandwidth can be obtained, corresponding to a much longer observation time after the Fourier transform [22,20].

In the time domain measurements a short picosecond pulse is needed in order to see the structure on a picosecond time scale. The width of this pulse is therefore determining the structure in the recurrence spectra that is observed. An experimental problem is the conservation of coherence in the pump-probe sequence. If the coherence of the atoms in the excited states is lost between the pulses, the interference effects will be lost as well.

Although great effort was taken to match the experimental conditions, minor differences are observed in this comparison probably caused by uncertainties in the experimental parameters such as electric field strength and laser wavelength. For the frequency-resolved measurements the electric field in which the atoms are placed is known within a 2% error. Slight changes in the electric fields cause some changes in the relative amplitudes of the recurrence peaks. The recurrence time also depends on the applied electric field. Furthermore, in the time-domain measurements the wavelength of the exciting short laser pulse was not as accurately known as the wavelength of the nanosecond dye laser. Broers *et al.* determined the laser frequency of the picosecond laser by scanning it over the saddle-point energy E_c and determining the half height of the ionization yield. The same procedure can be performed for the frequency-resolved measurements since we can convolute the spectra with a Gauss corresponding to the bandwidth of the picosecond laser, determine the half height of the ionization yield, and label this point E_c. In the case of perpendicular laser polarization a slight mismatch of 1.7% was found with the calculated saddle-point energy $E_c = -2\sqrt{F}$ for an electric field of 1.8 kV/cm. Throughout the article the calculated E_c is used.

In order to obtain the same experimental conditions the following procedure was followed. The electric field was varied to obtain the same recurrence times of the first and second recurrence. A deviation of 13% was found (1.8 kV/cm instead of 1.569 kV/cm). This deviation can be explained as follows. In the previously performed time domain experiment the electric field was not accurately defined due to the use of grids in the interaction zone instead of rigid plates. The electric field ratio is now fixed for all measurements. All the spectra from E_0 to E_c are now recorded for both polarizations. By multiplying these spectra by a Gaussian at positions $0.9E_c$, $0.79E_c$, $0.68E_c$, etc., and a width of 0.085 nm (FWHM), the spectra are obtained, which can directly be Fourier transformed to obtain the recurrence spectra.

V. COMPARISON WITH SCALED-ENERGY SPECTROSCOPY

In the frequency scans described in the previous sections the electric field strength is kept constant. For the technique of scaled-energy spectroscopy, the wavelength of the exciting laser as well as the electric field is scanned simultaneously to match the scaling criteria of the Hamiltonian describing the atom in the electric field. The Hamiltonian can be made field independent when the electric field strength F and excitation energy E are scaled according to [20]

$$F = \left(\frac{E}{\epsilon}\right)^2 , \tag{6}$$

TABLE I. Recurrence times in (picoseconds) from Figs. 4 and 5.

Energy	Parallel polarization		Perpendicular polarization	
(E_c)	Fourier	Time	Fourier	Time
0.22	4.6	4.6		
0.44	5.4	5.5	5.3	
0.67	6.2	6.0	5.9	5.8
0.79	6.4	6.4	6.3	6.3
0.90	6.8	6.7	6.8	6.7

where ϵ is the scaled energy ranging from 0 at E_0 to -2 at E_c. For $\epsilon = -2$ the electric field is scanned in such a way that the excitation always takes place at the saddle point E_c. The spectrum that is obtained is plotted as a function of $F^{-1/4}$ and Fourier transformed. The x scale of the Fourier transformed spectrum is given by the action S, which is defined as

$$S = \oint_P p \cdot dq \ , \tag{7}$$

where p is the momentum of the classical electron, q is the position of the electron, and the integration is over a periodic orbit of the electron [24]. The technique of scaled-energy spectroscopy was applied by Eichmann *et al.* [20] to the problem of a Rydberg atom in an electric field. Detailed theoretical have been performed by Gao and Delos [19] and a recent experimental study by Courtney *et al.* [25] suggests chaotic behavior of lithium Rydberg orbits below the saddle point. In Fig. 13 the recurrence spectra, at $\epsilon = -1.9$, obtained by Fourier transforming the frequency spectra, are plotted next to the scaled-energy spectra for various electric field strengths. Both the recurrence spectrum and the scaled-energy spectrum are obtained from the same frequency spectrum at a given field strength, allowing for a direct comparison.

The electric field is constant in these frequency scans, so the scaling criteria are not completely fulfilled. However, the spectral range that is Fourier transformed is sufficiently small to match the scaling criteria. For the different field strengths, the excitation is always at E_c. The first angular recurrence time in the recurrence spectra does strongly depend on the electric field, as can be seen in Fig. 6. At $\epsilon = -1.9$ the recurrence time scales as $\tau_{\rm rec} \sim F^{-3/4}$. For the scaled-energy spectra, the position of the peaks is independent of the electric field, showing that the scaling criteria are properly chosen.

In the scaled-energy spectra each peak can be assigned to a classical trajectory of the electron in the potential. These trajectories are calculated by Eichmann *et al.* [20] for hydrogen at $\epsilon = -2.5$. The simplest trajectory possible is given by an electron motion uphill in the $-z$ direction and back to the core. This trajectory gives a peak at $S = 0.425$ and can be compared to a radial wave packet. The bandwidth used to calculate these spectra is too small to excite a radial wave packet and is therefore not observed in these spectra. The action of $S = 2.4$ corresponds to angular wave packets, originating from a more complicated classical trajectory leaving the core at a shooting angle 176.6° at $\epsilon = -2.5$. These wave packets can be excited within the bandwidth used in these spectra and are indeed observed for all electric field strengths. After 40 ps the recurrence amplitude drops off rapidly due to the limited resolution of the experiment and the finite lifetime of the wave packet. For the scaled-energy spectra this upper limit is then a function of the electric field strength, as can be seen from the lack of higher action peaks for lower field strengths in Fig. 13.

We can transform the calculations by Eichmann *et al.* [20] ($\epsilon = -2.5$) to our case ($\epsilon = -1.9$) as follows. The angular recurrences scale as $\tau_k \sim \sqrt{\epsilon}$. The action axis, which is the inverse of the $F^{-1/4}$ axis, is proportional to $1/\sqrt{\epsilon}$. Therefore action peaks corresponding to angular recurrences are independent of ϵ. In contrast, for the radial recurrences the action peaks scale as ϵ^{-2}. In conclusion, the calculated actions for $\epsilon = -2.5$ ($S_{\rm rad} = 0.425$ and $S_{\rm ang} = 2.42$) are transformed to $S_{\rm rad} = 0.77$ and $S_{\rm ang} = 2.42$ at $\epsilon = -1.9$.

In Fig. 14 the scaled energy spectrum of rubidium in an electric field of 675 V/cm is shown. The conversion bandwidth is chosen to be larger such that both the scaled-action peak corresponding to a radial and an angular recurrence is observed. As can be seen in Fig. 14, the position of the peaks is in good agreement with the calculated values. Since the position of the peak corre-

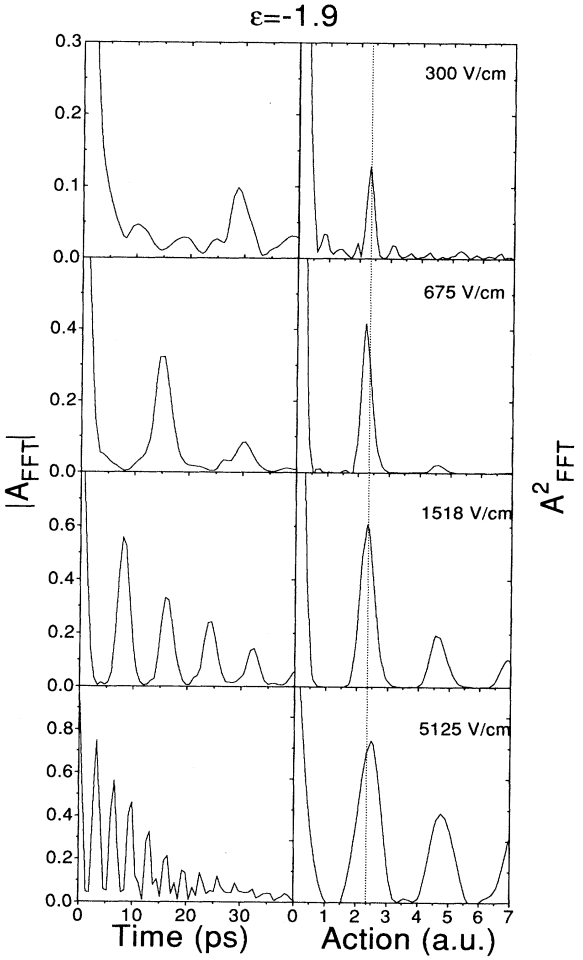

FIG. 13. Recurrence spectra at $\epsilon = -1.9$ as obtained by Fourier transforming the frequency spectrum are plotted in the left column, where $|A_{\rm FFT}|$ is the magnitude the Fourier transform. The laser polarization was chosen to be perpendicular to the electric field. In the right column the frequency spectra are transformed to scaled-energy spectra. To make this transformation the frequency spectra as a function of $F^{-1/4}$ are Fourier transformed and squared, i.e., $A^2_{\rm FFT}$. The dotted line at $S = 2.4$ corresponds to a classical trajectory in the potential.

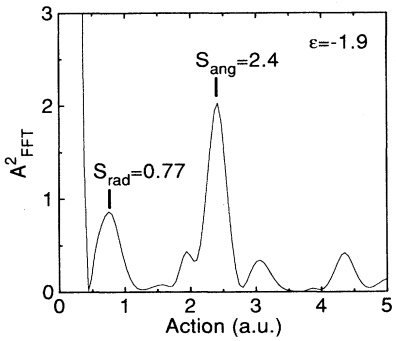

FIG. 14. Scaled-energy spectrum of rubidium in an electric field of 675 V/cm. The laser polarization was chosen to be parallel to the electric field. The spectral range that is Fourier transformed (0.18 nm FWHM) corresponds to to a range of $\epsilon = -1.8$ to $\epsilon = -2.0$. The vertical axis is given by the squared Fourier transform $A^2_{\rm FFT}$.

sponding to an angular recurrence is independent of the scaled energy ϵ, this peak is still observed in the scaled-action spectrum when the total frequency spectrum ranging from $\epsilon = 0$ to -2 is scaled and Fourier transformed. For the radial recurrence this is not the case due to the ϵ^{-2} scaling. When we increase the spectral range, i.e., increasing the range of ϵ, the radial recurrence peak is smeared out, whereas the angular recurrence peak at $S_{\rm ang} = 2.4$ remains present in the scaled-energy spectrum.

VI. CONCLUSIONS

We measured the ionization yield of rubidium atoms in an electric field. Fourier transforms of these spectra after multiplication with the spectrum of a short optical pulse allowed us to study the dynamics of wave packets above the classical field ionization limit. The dynamics of these wave packets was studied in detail as a function of the excitation energy between E_c and E_0, showing an oscillatory behavior of the amplitude of the recurrences as a function of the excitation energy. At given excitation energies the angular recurrence amplitudes were low because of the lack of blue Stark states in that energy region. For a complete understanding of the dynamics, both the frequency domain properties, such as n, k, and the wave-packet concepts, such as radial and angular oscillations, were required. Just above E_c long-lived states were observed with lifetimes up to microseconds. These long lifetimes allowed us to study these dynamics directly in the time domain. Instead of measuring the total ionization yield, the ionization yield as a function of time was measured.

Fourier transforms of the spectra were directly compared to the time-resolved experiments by Broers *et al.* [14], showing the analogy between the frequency and time resolved measurements. For the time domain measurements short optical pulses corresponding to a large bandwidth were needed, whereas in the frequency domain a small bandwidth was needed to resolve all the individual electronic states. Starting from the frequency domain, there was a large flexibility to synthesize recurrence spectra once the frequency spectrum had been recorded. For instance, a set of pump-probe experiments with various pulse durations can all be synthesized from a single spectrum. We conclude that Fourier transforming the frequency domain spectra is a preferred way to study the dynamics of an atomic electron in an electric field.

In addition, the scaled-energy spectra can be synthesized from the frequency spectra. Starting from the measured frequency spectrum we have studied both the time-dependent recurrence spectra as well as the scaled-energy spectroscopy spectra, allowing for a direct comparison. For the recurrence spectra the recurrence times were strongly dependent on the electric field, whereas in the scaled-energy spectra the action of the peaks did not change as a function of the electric field, which is a consequence of the scaling properties of the Hamiltonian. The simplest two trajectories at a scaled energy of $\epsilon = -1.9$ appeared at action values of $S = 0.77$ and $S = 2.4$. The actions of these trajectories correspond to radial and angular wave packets, respectively.

ACKNOWLEDGMENTS

The authors would like to thank B. Broers, J. F. Christian, J. H. Hoogenraad, H. B. van Linden van den Heuvell, R. B. Vrijen, and W. J. van der Zande for valuable discussions and careful readings of the manuscript. We thank A. Kips and W. Vassen for valuable discussion on scaled-energy spectroscopy. The work in this paper is part of the research program of the "Stichting voor Fundamenteel Onderzoek van de Materie" (Foundation for Fundamental Research on Matter) and was made possible by financial support from the "Nederlandse Organisatie voor Wetenschappelijk Onderzoek" (Netherlands Organization for the Advancement of Research).

APPENDIX: FREQUENCY DOMAIN VERSUS TIME DOMAIN

The time evolution of a wave packet in an electric field can be measured with a technique proposed by Noordam *et al.* [9] and used by Christian *et al.* [10]. A short laser pulse is used to excite a coherent superposition of Rydberg states, a wave packet. After a delay τ_d a second identical pulse is applied to the atoms. By varying the phase between the two pulses, interference giving rise to an enhancement or reduction of the Rydberg population occurs. This interference can occur only if the original wave packet has overlap with the wave packet created by the second pulse. By measuring the amplitude of the interference as a function of the delay between the two pulses, the recurrences of the wave packet to the core are probed. By measuring the root-mean-square value of the phase-dependent ionization yield, the overlap between the two wave packets, i.e., $|\langle\Psi(0)|\Psi(\tau)\rangle|$, is mea-

sured. The optical field of these two identical laser pulses with frequency ω_L, width τ_p, and delay τ_d can be written as

$$E(t) = E_0 \sin(\omega_L t) e^{-2\ln 2(t/\tau_p)^2} + E_0 \sin[\omega_L (t-\tau_d)] e^{-2\ln 2[(t-\tau_d)/\tau_p]^2} . \quad \text{(A1)}$$

Starting from the Schrödinger equation for hydrogen and applying the rotating-wave aproximation, we find for the amplitude of Rydberg state n

$$a_n(t) = -ie^{-i\omega_n t}\mu \int_{-\infty}^{t} dt' E(t') e^{-i(\omega_0-\omega_n)t'} , \quad \text{(A2)}$$

where μ is the matrix element $\langle 1s|z|np\rangle$ of the ground state and the excited Rydberg state and ω_0, ω_n are the energies of the ground state and the Rydberg state n, respectively. Introducing a lifetime Γ_n for each Rydberg state and the double pulse of Eq. (A1), the amplitude is given by

$$a_n(t) = A \int_{-\infty}^{t} dt' e^{-i\Delta_n t'} e^{-(\Gamma_n/2)(t-t')} \times [e^{-bt'^2} + e^{-b(t'-\tau_d)^2} e^{\omega_l \tau_d}], \quad \text{(A3)}$$

where $A = -iE_0 e^{-i\omega_n t}\mu$, $\Delta_n = \omega_0 - \omega_n + \omega_L$, and $b = 2\ln 2/\tau_p^2$. The integral can be solved analytically under the assumption that during the excitation pulse no population decay occurs, i.e., $\Gamma/2 \ll c$. The amplitude of the Rydberg state n, with lifetime Γ_n, directly after excitation with the double pulse at $t = \tau_d$ is then given by

$$a_n(\tau_d) = c_n e^{-i\omega_n \tau_d} (e^{-(\Gamma_n/2)\tau_d} + e^{i(\omega_n-\omega_0)\tau_d}) , \quad \text{(A4)}$$

where $c_n = -i\mu(\pi/2\ln 2)^{1/2}\tau_p E_0 e^{-(\Delta_n \tau_p)^2/8\ln 2}$.

We will now take a specific case in order to prove the analogy between the frequency- and time-resolved measurements in analytical form. We excite with a short laser pulse only two states at energies ω_1 and ω_2, both with lifetime Γ. Both states are populated equally, i.e., $c_1 = c_2 = c$. Substituting these values in Eq. (A4), we obtain, for the total population $P_{\text{time}}(\tau_d) = \sum_n |a_n|^2$,

$$P_{\text{time}}(\tau_d) = c^2 \left[2e^{-\Gamma\tau_d} + 2 + 4e^{-(\Gamma/2)\tau_d} \times \cos\left(\frac{\omega_1+\omega_2-2\omega_0}{2}\tau_d\right) \times \cos\left(\frac{\omega_1-\omega_2}{2}\tau_d\right)\right] . \quad \text{(A5)}$$

In the technique used to detect the population, only the amplitude of the fast oscillating terms is measured, i.e., the last term in Eq. (A6). The observable $P^*(\tau_d)$ is then given by

$$P^*_{\text{time}}(\tau_d) \sim c^2 e^{-(\Gamma/2)\tau_d} \left|\cos\left(\frac{\omega_1-\omega_2}{2}\tau_d\right)\right| . \quad \text{(A6)}$$

Starting from the frequency domain, the power spectrum can be written as a sum of Lorentzians, giving the resonnances with lifetimes Γ_n at energies ω_n

$$P_{\text{freq}}(\omega) = \sum_n \frac{c_n^2 \Gamma_n/2}{(\omega-\omega_n)^2 + (\Gamma_n/2)^2} , \quad \text{(A7)}$$

where c_n^2 is the cross section of state n. If we Fourier transform this spectrum we obtain

$$P_{\text{freq}}(t) = \sum_n c_n^2 \sqrt{\frac{\pi}{2}} e^{i\omega_n t} e^{-(\Gamma_n/2)t} . \quad \text{(A8)}$$

Taking two states with energies ω_1 and ω_2, $c_1 = c_2 = c$, $\Gamma_1 = \Gamma_2 = \Gamma$, and taking the magnitude of Eq. (A8) we obtain

$$P^*_{\text{freq}}(t) \sim c^2 e^{-(\Gamma/2)t} \left|\cos\left(\frac{\omega_1-\omega_2}{2}t\right)\right| . \quad \text{(A9)}$$

By comparing Eq. (A6) with Eq. (A9) we find that the expressions are equal. In conclusion, by Fourier transforming the frequency spectrum we can obtain the time-resolved recurrence spectrum. Note that the decay in amplitude is measured ($\Gamma/2$) instead of the population decay (Γ).

[1] M. L. Zimmerman, M. G. Littman, M. M. Kash, and D. Kleppner, Phys. Rev. A **20**, 2251 (1979).

[2] R. R. Freeman, N. P. Economou, G. C. Bjorklund, and K. T. Lu, Phys. Rev. Lett. **41**, 1463 (1978).

[3] W. L. Glab and M. H. Nayfeh, Phys. Rev. A **31**, 530 (1985).

[4] W. L. Glab and M. H. Nayfeh, Phys. Rev. A **31**, 3677 (1985).

[5] H. Rottke and K. H. Welge, Phys. Rev. A **33**, 301 (1986).

[6] T. F. Gallagher, *Rydberg Atoms*, 1st ed. (Cambridge University Press, Cambridge, 1994).

[7] A. ten Wolde, L. D. Noordam, A. Lagendijk, and H. B. van Linden van den Heuvell, Phys. Rev. A **40**, 485 (1989).

[8] A. ten Wolde, L. D. Noordam, A. Lagendijk, and H. B. van Linden van den Heuvell, Phys. Rev. Lett. **61**, 2099 (1988).

[9] L. D. Noordam, D. I. Duncan, and T. F. Gallagher, Phys. Rev. A **45**, 4734 (1992).

[10] J. F. Christian, B. Broers, J. H. Hoogenraad, W. J. van der Zande, and L. D. Noordam, Opt. Commun. **103**, 79 (1993).

[11] G. Raithel, H. Held, L. Marmet, and H. Walther, J. Phys.

B **27**, 2849 (1994).
[12] H. H. Fielding, J. Wals, W. J. van der Zande, and H. B. van Linden van den Heuvell, Phys. Rev. A **51**, 611 (1995).
[13] B. Broers, J. F. Christian, J. H. Hoogenraad, W. J. van der Zande, H. B. van Linden van den Heuvell, and L. D. Noordam, Phys. Rev. Lett. **71**, 344 (1993).
[14] B. Broers, J. F. Christian, and H. B. van Linden van den Heuvell, Phys. Rev. A **49**, 2498 (1994).
[15] I. Y. Kiryan and D. J. Larson, Phys. Rev. Lett. **73**, 943 (1994).
[16] Q. Wang and A. F. Starace, Phys. Rev. A **48**, 1741 (1993).
[17] J. Gao, J. B. Delos, and M. Baruch, Phys. Rev. A **46**, 1449 (1992).
[18] J. M. Mao, K. A. Rapelje, S. J. Blodgett-Ford, and J. B. Delos, Phys. Rev. A **48**, 2117 (1993).
[19] J. Gao and J. B. Delos, Phys. Rev. A **49**, 869 (1994).
[20] U. Eichmann, K. Richter, D. Wintgen, and W. Sandner, Phys. Rev. Lett. **61**, 2438 (1988).
[21] A. Holle, J. Main, G. Wiebusch, H. Rottke, and K. H. Welge, Phys. Rev. Lett. **61**, 161 (1988).
[22] T. van der Veldt, W. Vassen, and W. Hogervorst, Europhys. Lett. **21**, 903 (1993).
[23] R. R. Freeman and N. P. Economou, Phys. Rev. A **20**, 2356 (1979).
[24] M. C. Gutzwiller, Physica (Amsterdam) **5**, 183 (1982).
[25] M. Courtney, H. Jiao, N. Spellmeyer, and D. Kleppner, Phys. Rev. Lett. **73**, 1340 (1994).